EFDA–JET–CP(14)06/38

A.C.C. Sips, G. Giruzzi, S. Ide, C. Kessel, T.C. Luce, J.A. Snipes, J.K. Stober,
the Integrated Operation Scenario Topical Group of the ITPA
and JET EFDA contributors

Progress in Preparing Scenarios for ITER Operation

Progress in Preparing Scenarios for ITER Operation

A.C.C. Sips[1,2], G. Giruzzi[3], S. Ide[4], C. Kessel[5], T.C. Luce[6], J.A. Snipes[7], J.K. Stober[8], and the Integrated Operation Scenario Topical Group of the ITPA and JET EFDA contributors*

JET-EFDA, Culham Science Centre, OX14 3DB, Abingdon, UK

[1]JET-EFDA, Culham Science Centre, Abingdon, OX14 3DB, UK.
[2]European Commission, Brussels, Belgium.
[3]CEA, IRFM, F-13108 Saint-Paul-lez-Durance, France.
[4]Japan Atomic Energy Agency, 801-1 Muko-yama, Naka, Ibaraki 311-0193, Japan.
[5]Plasma Physics Laboratory, Princeton University, Princeton, USA.
[6]General Atomics, San Diego, USA.
[7]ITER Organization, F-13115 Saint-Paul-lez-Durance, France.
[8]Max-Planck-Institut für Plasmaphysik, D-85748, Garching, Germany.
** See annex of F. Romanelli et al, "Overview of JET Results", (25th IAEA Fusion Energy Conference, Saint Petersburg, Russia (2014)).*

Preprint of Paper to be submitted for publication in Proceedings of the 25th IAEA Fusion Energy Conference, St Petersburg, Russia
13th October 2014 - 18th October 2014

ABSTRACT

In recent years, dedicated experiments and coordinated scenario simulations, initiated by the Integrated Operation Scenarios Topical Group of the ITPA, have significantly advanced the preparation of ITER operation. This contribution will review the progress made. Plasma formation studies report robust plasma breakdown in devices with metal walls over a wide range of conditions, while other experiments use an inclined EC launch angle at plasma formation to mimic the conditions in ITER. For H-modes at q_{95}~3 many experiments have demonstrated operation with scaled parameters for the ITER baseline scenario at n_e/n_{GW}~0.85. Most experiments, however, obtain stable discharges at $H_{98(y,2)}$~1.0 only for $\beta_N = 2.0$-2.2. During the current rise, a range of plasma inductance ($l_i(3)$) can be obtained from 0.65 to 1.0, with the lowest values obtained in H-mode operation. For the rampdown, the plasma should stay diverted and maintain H-mode. For an ohmic rampdown a reduction of the elongation from 1.85 to 1.4 would minimise the increase in plasma inductance from 0.8 to 1.3-1.4. Simulations show that the proposed rampup and rampdown schemes developed since 2007 are compatible with the present ITER design for the poloidal field coils. ITER scenario development in hydrogen and helium requires high input power (>50MW). H-mode operation in helium may be possible at input powers above 35MW at a toroidal field of 2.65T, for studying H-modes and ELM mitigation. In hydrogen, H-mode operation is expected to be marginal, even at 2.65T with 63MW of input power. For a hybrid scenario at 12MA the code simulations give a range for $Q = 6.5–8.3$, using 30MW NBI and 20MW ICRH. For non-inductive operation at 7 – 9MA the simulation results show more variation. At high edge pedestal pressure (T_{ped} ~ 7keV) the codes predict $Q = 3.3–3.8$ using 33MW NB, 20MW EC and 20MW IC. Simulations using a lower edge pedestal temperature (~3keV) but improved core confinement obtain $Q = 5 – 6.5$, when ECCD is concentrated at mid-radius and ~20MW off-axis current drive (ECCD or LHCD) is added.

1. INTRODUCTION

The basic operational scenarios proposed [1] include the so-called baseline or reference scenario at 15MA and 5.3T (with $q_{95} = 3$). Second, the hybrid scenario targets a high neutron fluence mission at reduced plasma current (~12MA) with $Q = 5 – 10$ or high fusion gain, $Q \geq 20$, at 15MA [2]. Third, a steady-state scenario with $Q \sim 5$ at lower plasma currents (~9MA) with enhanced confinement and stability. Experiments in AUG, C-Mod, DIII-D, JET and JT-60U provide insight into the differences in operation and the results obtained in preparing ITER operating scenarios. Key parts of the ITER scenarios are determined by the capability of the proposed poloidal field (PF) coil set [3]. They include the plasma breakdown at low loop voltage, the current rise phase, the performance during the flat top phase and a rampdown of the plasma. The ITER discharge evolution has been verified in dedicated (joint) experiments. In recent experiments, the main focus of scenario studies has been the preparation of the baseline scenario and hybrid scenarios at high beta. Predictions for ITER operating scenarios have been developed for many years. Some of the scenario modelling has been coordinated by the “Integrated Operating Scenario” topical group (IOS-TG) of the International

Tokamak Physics Activity (ITPA). The goals of these integrated simulations are to establish a physics basis for the proposed operating modes in ITER, in conjunction with the results from recent tokamak experiments. Since it is not possible to reproduce all the physics parameters of ITER plasmas simultaneously in present experiments, simulations are used to project to ITER regimes using theory based physics models that are being tested against present tokamak experiments [4], [5] and [6].

2. DEMONSTRATING ITER SCENARIOS – PLASMA FORMATION

In ITER, the maximum toroidal electrical field for plasma formation is ~0.30 – 0.35 V/m. Experiments on JET [8], DIII-D [9], KSTAR [10] and Tore Supra (TS) [11] show that ohmic plasma startup with the electric field value of ITER (0.3V/m) is marginally possible for optimized magnetic field configurations. Data from existing machines at least do not show a clear size scaling of the electric field necessary for ohmic breakdown. Experiments with metallic (Be or high-Z) walls report no significant problems with plasma initiation, even after disruptions. However, with the Be-wall at JET sufficient gas fuelling was required during the plasma formation phase to avoid runaway electron build-up [12]. Assisting plasma startup by electron cyclotron heating (ECH) is highly desirable for ITER to increase the operational margin [13]. The relevance of ECH assistance is highlighted by the first experiments on KSTAR in 2008: ECH assistance was necessary to breakdown the first plasmas [14]. This access route to plasma formation was successively optimized and in 2010 even purely ohmic startup was achieved. A similar development route may be required in ITER [15]. One of the main aims of ECH is to provide input power for a more rapid increase in electron temperature to overcome the radiation barrier due to low-Z impurities. Dedicated experiments have been performed in present devices studying the ITER breakdown condition with ECH, including the effect of toroidal inclination of the EC beam, with the participation of the tokamaks AUG (using X2), DIII-D (X2), FTU (using O1), KSTAR (X2), Tore Supra (O1, X2), HL-2A (O1) and of the stellarator TJ-II (X2). All devices that participated in these dedicated experiments demonstrated ECH-assisted startup in the ITER-like mode, although in some cases the necessary power was almost a factor of 2 higher compared with perpendicular launch [13]. The DYON code is a plasma burn-through simulator developed at JET [16]. The simulation results have been compared and validated with experimental data from the JET campaigns with the ITER-like wall. The DYON code has also been used to perform a predictive simulation for ITER [17]. The simulation results indicate that Be impurity levels < 5 % should not impact on plasma burn-through in ITER.

3. DEMONSTRATING ITER SCENARIOS – PLASMA RAMPUP AND RAMPDOWN

For the 15MA baseline scenario in ITER, the current rampup for the baseline is anticipated to take from ~ 50 to 100s with an X-point formation at ~4MA after ~15s. The rampdown phase is predicted to take ~200s using diverted plasmas. Experimental activities on JET, DIII-D, C-Mod and ASDEX-U (AUG) were pursued from 2008–2012 to examine the rampup and rampdown phases

of the proposed ITER discharge [8]. For ohmic discharges, the plasma current rampup rates were varied in JET, C-Mod, AUG, and DIII-D, made to correlate with 60–100s rampup times in ITER, showing variations in $l_i(3)$ of 0.80–1.0 (faster-slower), while C-Mod showed a narrower range of 0.9–1.0. DIII-D could reach much lower values of li to 0.65, but these became MHD unstable. With additional heating in the rampup, l_i is observed to be lower or similar to ohmic by the end of the rampup phase. If the heating leads to an H-mode transition during the rampup even lower l_i ~0.65 are reached, as well as some further reduction in the resistive consumption [8]. Overall, experiments have indicated that the ITER baseline discharge should have the capability to keep the l_i value within a range that is vertically stable, by utilizing a large bore plasma following breakdown, by diverting as early as allowed by the PF coils and heating in L-mode.

The rampdown phase in ITER has to reliably terminate the discharge, either from a scheduled end to burning plasmas or when it is necessary to stop the discharge following a request from the control systems. To allow maximum burn duration, no addition flux should be used during the rampdown phase. The reduction of the plasma current should be controlled and slow enough to avoid the plasma inductance from increasing to levels where it is not possible to maintain control over the vertical position of the plasma. Typically, the fusion power will reduce during the current rampdown, leading to a (sudden) H to L back transition, which leads to difficulties with controlling the radial position of the plasma. C-Mod [18], DIII-D [19], [20] and JET [21] produced a range of rampdown experiments, and each reduced elongation from 1.7–1.8 down to ~1.4–1.5 while maintaining lower divertor configuration. The combination of elongation reduction and current rampdown rate should be used to provide a stable rampdown phase. The H-mode can be robustly maintained into the rampdown at least to 2/3–1/2 of the flattop plasma current, thereby avoiding a CS over-current near the maximum CS current at end of flattop. The plasma density was found to decrease, keeping n_e/n_{GW} fixed, regardless of the plasma current ramp rate.

4. OPERATING EXPERIENCE AT CONDITIONS REQUIRED FOR Q ~ 10 IN ITER

Experience in present-day experiments (C-Mod, AUG, DIII-D, and JET) with the baseline scenario show conditions suitable for Q = 10 in ITER can be achieved. Figure 1 shows an example from the DIII-D tokamak [22]. The most stable operating region found to be $\beta_N \sim 2$. Similar plasmas are obtained in JET [23], AUG [24] and C-Mod [18] across a broad range in plasma density. Heating methods that do not apply torque have been used in C-Mod, JET (both with ICRF) and AUG (ECH and ICRF). The limited data in the baseline scenario show little change in the H factor when RF is used as main heating. Reducing the torque to ITER relevant levels does lead to a narrowing of the stable operating range in DIII-D and a small reduction in H-factor. Operation experience with High-Z wall materials is progressing. Demonstration of the ITER reference scenario on AUG with its tungsten wall has been performed using central wave-heating (ECH or ICRF) to avoid core tungsten impurity accumulation [24]. Stable behaviour for many confinement times has been obtained at $n_e/n_{GW} = 0.80–0.85$ and energy confinement ($0.95 \leq H_{98(y,2)} < 1.05$) as long as β_N stayed

above 2 (typically $2.0 < \beta_N < 2.2$). With the carbon wall in JET, baseline ELMy H-mode plasmas ($q_{95} = 3–3.6$, $\beta_N \sim 1.2–1.6$) achieved good normalised confinement with $H_{98(y,2)} \sim 1$ in unfuelled plasmas. In recent experiments with the ILW, gas fuelling is required to avoid W contamination [25]. The low triangularity plasmas showed a similar degradation due to the fuelling as in JET-C. However, the good confinement in JET-C for the high triangularity plasmas could not be sustained in JET-ILW at high gas levels; a 20–30 % reduction in pedestal and, through profile stiffness, core confinement was observed. The confinement improves at higher beta values ($\beta_N \geq 2$) such that the hybrid scenario at JET shows no difference in overall confinement compared to carbon wall results [26]. Experiments in AUG and JET [25] with nitrogen gas puffing and AUG [24] with CH4 puffing show the pedestal can return to the higher level seen with the graphite wall despite enhanced radiation. One common theme from these experiments is that is it difficult to obtain stable, stationary conditions when the loss power is just above the power threshold for entering H mode; ELMs become infrequent, leading to a rise in the electron density and, in devices with metal walls, a rise in the impurity density and core radiation.

5. HYBRID (ADVANCED INDUCTIVE) OPERATION AT HIGH PERFORMANCE

Over the last decade, inductive scenarios (mainly at $q_{95} = 4$) capable of higher normalized pressure ($\beta_N \geq 2.4$) than the ITER baseline scenario ($\beta_N = 1.8$) with normalized confinement at or above the standard H-mode scaling are well established under stationary conditions on the four largest diverted tokamaks (AUG, DIII-D, JET, JT-60U). A database of more than 500 plasmas from these tokamaks has been analysed [2], showing that the parameter range for which high performance is achieved is broad; both in q95 (as shown in figure 2) and density normalized to the empirical density limit. Although some uncertainty remains, it appears that the stationary current profile, with q(0) near 1 but with flat magnetic shear in the centre observed at $q_{95} \sim 4$ and $\beta_N \sim 2.5–3.5$ yields both improved stability to tearing modes and improved confinement. In addition to opening the operating space, the reduced plasma current and increased β_N lead to the possibility of much longer pulse operation at Q~10 in ITER, approaching an hour, due to the higher temperature reducing the resistivity and the increased bootstrap current, both reducing the flux required to supply the inductive magnetic energy.

6. PROGRESS IN SCENARIO MODELLING - ITER BASELINE OPERATING SPACE

The poloidal field coil system on ITER is a critical element for achieving mission performance. Analysis of PF capabilities has focused on the operating space available for the 15MA Q = 10 scenario. Simulations have been performed using three free-boundary transport simulation codes, TRANSP/TCS [41], CORSICA [32] and DINA. The simulations use a prescribed density profile evolution and the Coppi-Tang [27] thermal transport model to evolve the plasma for the baseline 15MA inductive scenario. Prior to the rampup phase, the plasma will be initiated followed by an early startup phase, where about 20Wb are used to initiate the plasma and bring the plasma current to ~0.5MA. The entire rampup from 0.5 to 15MA, with additional heating, can require between 190 and 225 Wb

depending on a number of features such as the energy confinement, heating level and heating type, whether an H-mode is induced, and the rampup time. The flattop phase requires 30–40Wb to sustain the high temperature plasma for ≥ 300s. The CS coils will be near their current/field limits at the end of the flattop phase. Simulations indicate an over-current of the central solenoid coils if the plasma transitions from H to L-mode at the end of the flattop phase, due to the sudden inward motion of the plasma. As experiments have shown, maintaining the plasma in H-mode when entering the rampdown phase and sustaining it sufficiently long (roughly 1/3 to 2/3 into the rampdown) avoids this response in the central solenoid coils. The time-dependent simulations performed, represent the present state-of-the-art in producing scenarios representative of experimental conditions and show that the requirements for the PF coils are consistent with the operating space boundaries set by maximum allowed coil currents and forces. The results for 15MA are summarised in Figure 3 [28]. Recently, simulations show that long pulse (> 1000s) operation of ITER at 13–15MA is possible at low plasma density ($<n_e>/n_{GW}$ ~0.5) and Q~5. These simulations [29] take into account the predicted values of the separatrix temperatures and densities, Ts, ns, by the SOLPS code [30]. In contrast with standard pedestal assumptions, the inclusion of SOLPS predicts no degradation of the pedestal pressure with density. Hence, at lower density, higher electron temperature increases the NB and EC driven currents and reduces the resistive loss, thus allowing longer pulse operation in these conditions than for the reference 15MA at Q = 10. Various codes and transport models have been used for the predictions of burn duration in these conditions, giving good agreement [29]. These types of discharges could provide neutron fluence for TBM tests.

7. MODELLING NON-ACTIVE OPERATION IN ITER

A non-active phase of operation is planned for the first few years of operation in ITER. For hydrogen operation in ITER the maximum input power will be in the range 53–63 MW, depending on the use of the 3He minority ICRF heating scenario. For helium operation 63MW will be available. To limit the (hydrogen) NBI shine-through power to the first wall (< 4 MW/m^2), NBI can only be used above 4.5×10^{19} m^{-3} electron density in pure hydrogen and 2.5×10^{19} m^{-3} in helium. In preparation for operation in hydrogen and helium, several simulations have been performed with CORSICA [32] and JINTRAC [33]. Key in these simulations is the access to H-mode, without the α-heating from DT reactions. Simulations for hydrogen at 15MA and 5.3T and 63MW heating power, remain in L-mode even at the lower prescribed L-mode density of $<n_e> = 0.5n_{GW}$. Moreover, after only 20–50s of flat top at 15MA the central solenoid current limit is reached. Helium plasmas at 15MA, 5.3T may obtain a dithering H-mode at maximum input power with brief H-mode phases dropping back to L-mode due to the density rise during the H-mode phase. So, given the nominally available heating power of 63MW, it is unlikely that ITER can achieve robust H-mode operation in hydrogen or helium at 5.3T. At 7.5MA and 2.65T, the required heating power in hydrogen at low plasma density ($0.5n_{GW}$) is close to the L-H threshold power and a small reduction in the available power will drop the plasma into a poor quality H-mode. The simulations show that there is no limit to the

CS coils or PF coils for a flat top length of 200s at 7.5MA (even in L-mode). For helium operation, H-mode may be possible down to a power level of 35 MW suggesting sufficient margin for H-mode operation. At 7.5MA, 2.65T helium plasmas are predicted to reach good type-I ELMy H-mode conditions with $T_{i,ped} \sim 3700$eV, $T_{e,ped} \sim 3500$eV. Using JINTRAC, predictions for helium operation at 7.5MA and 2.65T have been optimised showing that the flat top could be extended beyond 300s.

8. BENCHMARKING HYBRID AND STEADY-STATE SIMULATIONS

In order to provide more consistent predictions for ITER, common sets of parameters for scenario simulations and a comparison (benchmarking) of the various codes has been coordinated by the IOS-TG since 2005. These activities involve the comparison of 1.5D core transport modelling assumptions and source physics modelling assumptions. The simulations focus on code to code results when using the same energy transport model, and within the same code when using different energy transport models. Five 1.5D transport evolution codes (including either fixed or free-boundary equilibrium computation) have been involved in simulations for ITER: ASTRA [34], [35], CRONOS [36], ONETWO [37], FASTRAN [38], TOPICS-IB [39], [40] and TSC/TRANSP [41]. Initially, a set of parameters of an ITER hybrid scenario at 12MA and the heat transport model GLF23 [42] have been chosen. In this exercise, the injected powers are limited to the negative ion NBI (1MeV, 33MW, steered to full off-axis) and ICRF heating (20MW, 53MHz, 2nd T harmonic). For these simulations the pedestal parameters are specified as $\rho_{ped} = 0.925$, $n_{ped} = n(\rho = 0.925) = n(0) = 0.85 \times 10^{20}$ m^{-3}, T_{ped} is set to 5keV. Simulations have been performed limited to the evolution of current and temperature profiles (i.e., with non-evolving density, rotation and impurity profiles). An overview of the parameters obtained is given in Table 1. The five codes globally provide a similar description of the main properties of the scenario. The confinement enhancement factor ranges from 1.07 to 1.23, with normalised beta from 2.1 to 2.4 giving a range for the prediction of the fusion gain of 6.5–8.3. Nevertheless, substantial differences were observed in the heat sources profiles (α-power, NBI and ICRH), as well as in the implementation of the GLF23 heat transport model (use of pressure stabilization term, rotation stabilization features, and approaches used to stabilize the algorithm). In addition, there are still some discrepancies in the computed radiation losses for the hybrid simulations (including a possible over/under counting of bremsstrahlung and line radiation). Several, more detailed, benchmark studies were performed to resolve these issues. The NBI deposition profiles have been the object of a separate benchmark exercise on NBI codes [43], [44], not summarised in this paper. The benchmark exercise was extended to steady-state scenarios [6]. Steady state operation in ITER can be obtained by (1) operating at high edge pedestal pressure, with $T_{ped} \sim 7$keV at 8–9MA or (2) at lower edge pedestal pressure ($T_{ped} \sim 3$keV) but with internal transport barriers (ITBs) at normalized pressures close to the ideal no-wall limits [47], [48]. A weak magnetic shear, at $I_p = 8$MA and a pedestal temperature $T_{ped} \sim 7$keV has been analysed with six scenario codes, using ITER day-1 heating systems and a GLF23 transport model. Figure 4 shows the comparison of the profiles calculated by the codes, showing good agreement. The total current

densities are in excellent agreement, with some differences in edge current (mainly determined by the bootstrap contribution). The confinement enhancement factor ranges from 1.3 to 1.5, with normalised beta from 2.3 to 2.8 giving a range for the prediction of the fusion gain (Q) of 3.3–3.8. Code comparison in ITB steady-state scenarios has been found to be much more challenging. A steady-state scenario [45] characterized by an ITB at mid-radius, purely RF current drive and 75% of bootstrap fraction, was originally computed with CRONOS. In these simulations, the pedestal temperature is fixed at $\rho \sim 0.93$ at a value of $T_{ped} \sim 3$keV. The simulations show that the plasma forms a stationary ITB when EC is deposited at $\rho = 0.45$ at power levels 12–20MW. The ECCD locks the ITB at mid-radius and this scenario has been used as a test case for CRONOS, ONETWO/FASTRAN and TOPIC-IB. However, the resultant temperature and q profiles are different for the three codes, requiring further study.

9. EXPLORING OPTIONS FOR ADVANCED SCENARIOS IN ITER

Insight to the achievability of steady state operation in ITER has been obtained from simulating a range of scenarios at reduced plasma current (7MA–10MA) at 5.3 T. At these levels of plasma current, the necessary plasma confinement for obtaining $Q \sim 5$ is in the range $H_{98(y,2)} = 1.3–1.7$ [46]. Predictions for steady state operation in ITER with weak-shear in the centre have been used to optimise the heating and current drive systems for ITER. In these simulations, an edge profile scaled from that of an ITER steady state demonstration in DIII-D [49] was adopted near the boundary ($\rho = 0.8–1.0$). The operating current and field are $I_p = 8$MA and $B_T = 5.3$T. The top of the pedestal is set at $\rho ped = 0.91$ with $\beta_N = 1.20$ at the top of the pedestal (resulting in the aforementioned Tped = 7keV). The q-profile (and low shear in the core) obtained is strongly determined by the edge bootstrap current. For the day-1 reference H&CD mix shows that operation at higher I_p (e.g. 9MA) would be important to reach $Q \sim 5$ objective. The high pedestal pressure provides bootstrap current at a level of 50–60% of the total plasma current. Neutral beam injection provides 2–3MA of non-inductive current drive and ECCD provides a modest 0.6–0.9MA. A steady-state scenario characterized by an ITB at mid-radius, and $T_{ped} \sim 3$keV has also been used in an assessment of the heating and current drive system requirements for non-inductive operation in ITER. In addition, ideal MHD stability has been analysed for variations of the Greenwald fraction and of the pressure peaking factor around the operating point. Several combinations of heating and current drive sources have been used in fully non-inductive scenario simulations for plasma currents in the range 7–10MA [7], using the Tokamak Simulation Code (TSC) [50] coupled with TRANSP [51] to provide models for the heating and current drive sources. It is found that 73 MW of heating power (20MW IC and 20MW EC combined with 33MW NB), as planned for the initial operations on ITER, can sustain up to 7.4MA of non-inductive current in the flat-top. This scenario has a fusion gain of $Q = 2–3.5$, operates at $\beta_N \leq 2.4$ and is predicted to be ideal MHD stable for variations of the plasma parameters around the operating point. Different heating upgrade options are under consideration for ITER [52]. Using an additional 20 MW of EC increases the non-inductive EC current to 1.5MA with

Q ~3.4 and β_N ~ 2.4 at 8.8MA. A combination of 20MW EC and LH has better performance with Q = 5 and minimum safety factor above 1.5.

CONCLUSIONS

In recent years, dedicated experiments and coordinated scenario simulations, initiated by the Integrated Operation Scenarios Topical Group of the ITPA, have significantly advanced the preparation of ITER operation. The experiments cover a wide range of topics such as plasma formation, plasma rampup and reliable rampdown, the demonstration of the ITER baseline and alternatives to achieve the ITER goal of Q = 10 at 500MW of fusion power. Scenario simulations have been benchmarked and provide insight to the requirements for achieving long sustained burn, steady state operation and early operation in hydrogen and helium. Several issues remain to be studied, including plasmas with dominant electron heating, mitigation of transient heat loads integrated in scenario demonstrations and (burn) control simulations [53] in ITER scenarios.

ACKNOWLEDGEMENTS

The authors wish to thank the ITER-IO, and in particular the EFDA contributors, the ASDEX-Upgrade team, the DIII-D team and the C-Mod team. The views and opinions expressed herein do not necessarily reflect those of the ITER Organization.

REFERENCES

[1]. M. Shimada et al, Nuclear Fusion **47** (2007)
[2]. T.C. Luce et al, Nuclear Fusion **54** (2014) 013015
[3]. C.E. Kessel et al, Nuclear Fusion **49** (2009) 085034
[4]. T. Casper et al, Proc. 24th FEC, San Diego, USA (2012) ITR/P1-15
[5]. C.E. Kessel et al, Nuclear Fusion **47** (2007) 1274
[6]. M. Murakami et al, Nuclear Fusion **51** (2011) 103006
[7]. F.M. Poli et al, Nuclear Fusion **52** (2012) 063027
[8]. A.C.C. Sips et al, Nuclear Fusion **49** (2009) 085015
[9]. B. Lloyd et al, Nuclear Fusion **31** (1991) 2031
[10]. Jayhyun Kim et al, Nuclear Fusion **51** (2012) 083034
[11]. J. Bucalossi et al, Proc. 22nd FEC, Geneva, Switzerland (2008) EX/P6 – 12
[12]. P.C. de Vries et al, Nuclear Fusion **53** (2013) 053003
[13]. J. Stober et al, Nuclear Fusion **51** (2011) 083031
[14]. Y.S. Bae et al, Nuclear Fusion **49** (2009) 022001
[15]. B. Lloyd et al, Plasma Phys. Control. Fusion **38** (1996) 1627
[16]. Hyun-Tae Kim et al, Nuclear Fusion **52** (2012) 103016
[17]. Hyun-Tae Kim et al, Plasma Physics and Controlled Fusion **55** (2013) 124032
[18]. C.E. Kessel et al, Nuclear Fusion **53** (2013) 093021

[19]. G. L. Jackson et al, Physics of Plasmas **17** (2010) 056116; doi: 10.1063/1.3374242
[20]. P.A. Politzer et al, Nuclear Fusion **50** (2010) 035011
[21]. A.C.C Sips et al, Proc. 23rd FEC, Daejeon, Rep. of Korea (2010) EXC/P2-08
[22]. G.L. Jackson et al, Proc. 24th FEC, San Diego, USA (2012) EX/P2-08
[23]. A.C.C. Sips et al, Proc. 24th FEC, San Diego, USA (2012) ITR/P1-11
[24]. J. Schweinzer et al, 40th EPS Conference, Espoo, Finland (2013) P2.134
[25]. M.N.A. Beurskens et al, Proc. 24th FEC, San Diego, USA (2012) EX/P7-20
[26]. C.D. Challis et al, this conference, EX/9-3
[27]. W.M. Tang, Nuclear Fusion **26** (1986) 1605
[28]. T. Casper et al, Proc. 23rd FEC, Daejeon, Rep. of Korea (2010) ITR/P1-19
[29]. A.R. Polevoi et al, this conference, PPC/P3-2
[30]. D.P. Coster et al, Proc. 19th FEC, Lyon, France, (2002) TH/P2-13
[31]. A.S. Kukushkin et al, Nuclear Fusion **45** (2005) 608
[32]. J.A. Crotinger et al, LLNL Report UCRL-ID-126284 (1997) NTIS #PB2005-10215
[33]. S. Wiesen, JET Report (2008), http:/ /www.eirene.de/JINTRAC_Report_2008.pdf
[34]. G. Pereverzev et al, IPP Report 5/98 (2002)
[35]. Yong-Su Na et al, Nuclear Fusion **49** (2009) 115018
[36]. J.F. Artaud et al, Nuclear Fusion **50** (2010) 043001
[37]. H. St. John et al, Proc. 15th FEC, Seville, Spain (1994) Vol. 3 p. 603
[38]. J.M. Park et al, Proc. 23rd FEC, Daejeon, Rep. of Korea (2010) EXC/P2-05
[39]. H. Shirai et al, Plasma Physics and Controlled Fusion **42** (2000) 1193
[40]. N. Hayashi et al, Nuclear Fusion **45** (2005) 933
[41]. C.E. Kessel et al, Physics of Plasma **13** (2006) 056108
[42]. J.E. Kinsey et al, Physics of Plasmas **12** (2005) 052503
[43]. T. Oikawa et al, Proc. 22nd FEC, Geneva, Switzerland (2008) IT/P6-5
[44]. M. Schneider et al, Nuclear Fusion **51** (2011) 063019
[45]. J. García et al, Physical Review Letters **100** (2008) 255004
[46]. T.C. Luce, 1st IOS-TG meeting, 20 October 2008 (2008)
[47]. Y. Shimomura et al, Plasma Physics and Controlled Fusion **43** (2001) A385
[48]. B.J. Green, Plasma Physics and Controlled Fusion **45** (2003) 687 – 706
[49]. E.J. Doyle et al, Nuclear Fusion **50** (2010) 075005
[50]. S.C. Jardin, et al, Journal of Computational Physics **66** (1986) 481
[51]. R.J. Hawryluk et al, Physics of Plasmas Close to Thermonuclear Conditions, vol 1 (1980) 19–46
[52]. D. Bora et al, 17th Top. Conf. on RF Power in Plasmas, Clearwater, Florida (2007) pp. 25-32
[53]. C.E. Kessel, this conference, PPC/P3-19

	ONETWO	TOPICS	TSC/TRANSP	CRONOS	ASTRA
$T_e(0)$ (keV)	27.2	31	33.8	26.3	33.5
$T_i(0)$ (keV)	33.4	32.3	33.8	25.6	32.3
I_{BS} (MA)	3.87	3.83	3.39	4.26	2.89
I_{NB} (MA)	2.07	2.26	1.42	0.92	1.91
I_{EC} (MA)	-	-	-	-	-
f_{NI}	0.50	0.51	0.40	0.43	0.40
Q	6.5	7.7	7.5	8.3	7.9
P_α (MW)	69	82	80	87.6	83.3
β_N	2.1	2.38	2.18	2.3	2.07
$H_{98(y,2)}$	1.1	1.07	1.18	1.23	1.2
q(0)	0.58	0.50	0.44	0.69	0.43

Table 1. Scalar parameters for the benchmarking of the hybrid scenario at 12 MA, 5.3 T, using the GLF23 transport model in five different scenarios codes. [5].

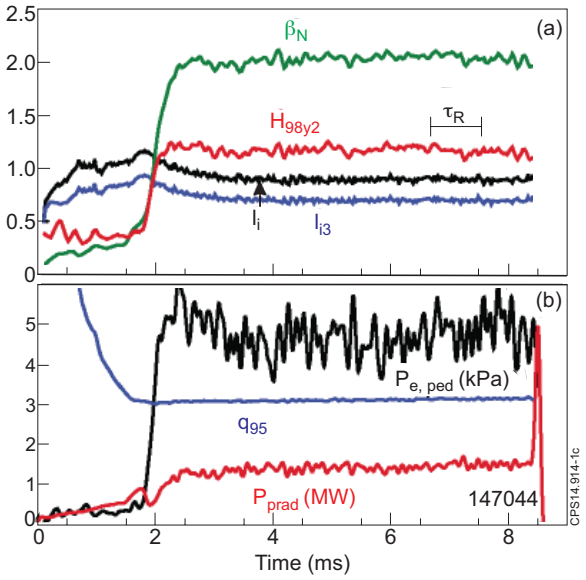

Figure 1: Demonstration of baseline scenario to resistive equilibrium in DIII-D [22].

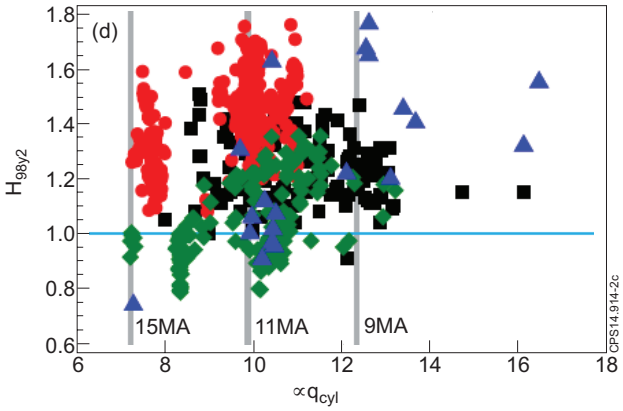

Figure 2: Advanced inductive plasmas achieve stationary high performance across a broad range of q_{95} [2].

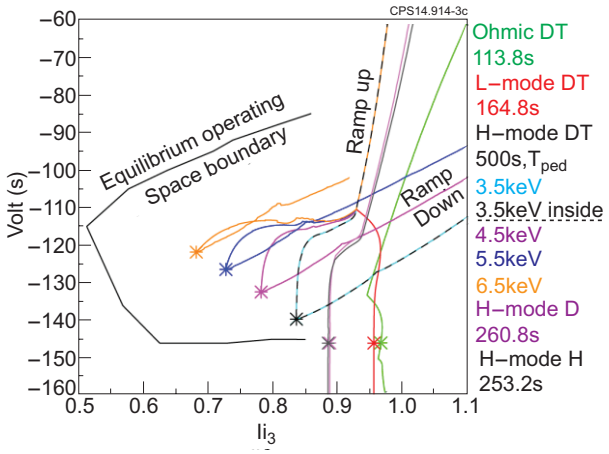

Figure 3: Mapping of the operating space in ITER with the various different assumptions for the current rise phase and edge pedestal temperature for the flat top phase [28].

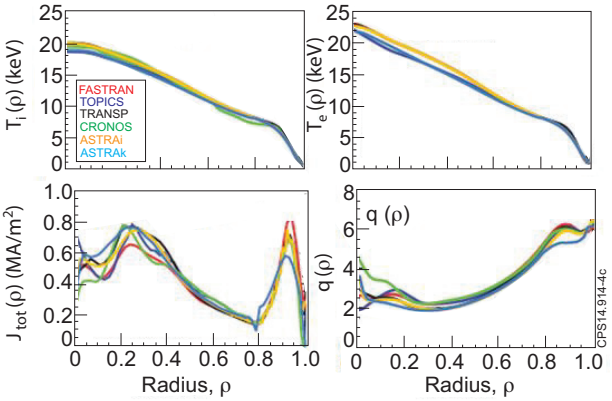

Figure 4: Weak shear steady-state scenario: comparison of ion temperatures (top left), electron temperatures (top right), current densities (bottom left), safety factors (bottom right) computed by different codes [6].